J. Phys. B: At. Mol. Opt. Phys. **29** (1996) 2115–2125. Printed in the UK

Elastic and excitation cross sections for electron–nitrous oxide collisions

S E Michelin†, T Kroin† and M T Lee‡

† Departamento de Física, Universidade Federal de Santa Catarina, 88049 Florianópolis, SC, Brazil

‡ Departamento de Química, Universidade Federal de São Carlos, 13565-905 São Carlos, SP, Brazil

Received 31 October 1995

Abstract. In this work, we present a theoretical study of elastic and inelastic electron–N_2O collisions in the low and intermediate incident energy range. More specifically, we report differential and integral cross sections for the elastic scattering in the 5 to 80 eV range as well as the excitation cross sections for the transitions leading to the lowest $^1\Pi$ and $^3\Pi$ states in the 10 to 100 eV range. The Born-closure Schwinger variational method was applied for the elastic scatterings whereas the distorted-wave method was used to study the electron impact excitation processes. The calculations were carried out using the fixed-nuclear static-exchange approximation at the equilibrium geometry of the ground-state N_2O. The comparison between the calculated results and the available experimental data in the literature is encouraging.

1. Introduction

Elastic and electronic excitation cross sections for electron scattering by atoms and molecules are of fundamental importance in a great variety of physical and chemical processes and thus their determination has been a subject of continuously increasing interest for both experimentalists and theoreticians working in this field (Trajmar *et al* 1983). Nitrous oxide (N_2O) is a particularly interesting molecule and has attracted increasing attention probably due to its participation in a number of processes. For example, nitrous oxide has been found to be important in the chemistry of the upper atmosphere where it may play roles in the destruction of the ozone layer (Hahn and Junge 1977, Wang and Sze 1980, Wayne 1991). Also, N_2O lasers have been used as a secondary standard in areas of spectroscopy within the 10 μm region where the frequency of CO_2 lasers is inadequate (Fox and Reid 1985). From a scientific point of view, N_2O is isoelectronic of CO_2 and both molecules are linear in the ground states, therefore, it is expected that the electron scattering cross sections by these molecules are similar, although N_2O has a weak dipole moment and CO_2 has not. Indeed, the similarity in the elastic electron collisions by both molecules was confirmed recently by Johnstone *et al* (1993).

In the past fifteen years, several measured cross sections for electron scattering from N_2O have been reported. Kwan *et al* (1984) and Szmytkowski *et al* (1984, 1989) measured total cross sections and Kubo *et al* (1981), Marinković *et al* (1986) and more recently Johnstone *et al* (1993) have published differential cross sections (DCS). The vibrational DCS for incident energies in the 2 and 8 eV regions were reported by Azria *et al* (1975), Tronc *et al* (1981) and Andrić and Hall (1984). Recently, Barnett *et al* (1991) reported the

0953-4075/96/102115+11$19.50

observation of metastable N_2 and O from electron impact dissociative excitation of N_2O. For the electronic excitation of N_2O by electron impact, the experimental data referring the excitation to the $^1\Pi$ and $2^1\Sigma^+$ states were reported by Marinković *et al* (1986).

In contrast to the numerous experimental activities, to date, there has been only one reported theoretical study, the calculation of the vibrational excitation cross sections at low incident energies (Dubé and Herzenberg 1975), in the literature.

In this work, we present for the first time a theoretical study of elastic and inelastic electron scattering by the N_2O molecule. More especifically, we report the elastic differential and integral cross sections in the energy range of 5–80 eV and also the excitation cross sections for the transitions from ground state to the first $^3\Pi$ and $^1\Pi$ ($2\pi \rightarrow 8\sigma$) states in the 10 to 100 eV range. For elastic scattering, we used the Born-closure Schwinger variational method (BCSVM, Lee *et al* 1990) whereas the electron-impact excitation cross sections were calculated using the distorted-wave approximation (DWA, Fliflet and McKoy 1980, Lee *et al* 1990). The BCSVM has already been applied to calculations of elastic electron scattering cross sections for a number of linear (Lee *et al* 1990, 1992) and non-linear molecules (Machado *et al* 1995a, b). It has been found that the BCSVM can provide quite reliable cross sections in the intermediate energy range. On the other hand, the DWA is a computationally simple method. Previous work (Lee and McKoy 1983, Lee *et al* 1995) has shown that in general the DWA can describe the angular distribution of the differential cross sections quite well although it overestimates the magnitude of the cross sections by a factor of 2 to 3. However, the reliability of the calculated cross sections increases with increasing incident energy. Therefore, the use of DWA as a first study for electron impact excitation of N_2O is suitable.

The organization of this paper is as follows: in section 2, we describe briefly the theory used and also some details in calculations. In section 3 we compare our calculated results with available experimental data and discussions.

2. Theory and calculation

Since the detail of the BCSVM and DWA have already been presented in previous works, here we will only outline briefly the theory used. After carrying out the average of the molecular orientation, the j_t basis representation (Fano and Dill 1972) of the laboratory-frame (LF) differential cross section (DCS), for both elastic and inelastic electron–N_2O scattering is given by

$$\frac{\mathrm{d}\sigma}{\mathrm{d}\Omega}(n \leftarrow 0) = SM_n \frac{k_f}{k_0} \sum_{j_t m_t m_t'} \frac{1}{(2j_t+1)} \mid B^{j_t}_{m_t m_t'}(n \leftarrow 0, k_0, k', \hat{r'}) \mid^2 \qquad (1)$$

where $\boldsymbol{j_t} = \boldsymbol{l'} - -\boldsymbol{l}$ is the transferred angular momentum during the collision, m_t' and m_t are the projections of j_t along the laboratory and molecular axis, respectively. The S factor results from summing over final and averaging over initial spin sublevels, and M_n is the orbital angular momentum projection degeneracy factor of the final target state. k_0 and k_f are the momenta of the incoming and outgoing electron, respectively. In equation (1), $B^{j_t}_{m_t m_t'}$ is the coefficient of the j_t-basis expansion of the LF-scattering amplitudes and is given by

$$B^{j_t}_{m_t m_t'}(\Omega') = \sum_{l'lm'm} (-1)^m a_{ll'mm'}(ll'0m_t \mid j_t m_t)(ll'mm' \mid j_t m_t')Y_{lm_l}(\Omega') \qquad (2)$$

where the dynamical coefficients $a_{ll'mm'}$ for the transition from a initial target state $|0\rangle$ to a final target state $|n\rangle$ can be written in terms of fixed-nuclei partial-wave components of the

electronic portion of the transition matrix elements as

$$a_{ll'mm'}(n \leftarrow 0, k_0) = -\tfrac{1}{2}\pi[4\pi(2l'+1)]^{1/2}\mathrm{i}^{l'-l}\langle k_f lm, n \mid T \mid k_0 l'm', 0\rangle. \tag{3}$$

For elastic scattering, the reactance K-matrices were calculated in the static-exchange approximation using the Schwinger variational iterative method (SVIM Lucchese *et al* 1982). The transition T-matrices are related to the K-matrices through the expression

$$T = -\frac{2\mathrm{i}K}{(1-\mathrm{i}K)} \tag{4}$$

On the other hand, the distorted-wave approximation (DWA) is used to calculate the T-matrices for the electron-impact molecular excitation processes. In this case, both the incident and scattered continuum waves, distorted by the static-exchange potential field of the ground-state target, were also calculated using the SVIM. This calculation scheme makes our DWA equivalent to the first-order many-body theory (Csanak *et al* 1971) and, as pointed out by Rescigno *et al* (1974), this scheme is expected to incorporate the most important effects in calculation of the excitation transition matrix.

The electronic configuration of the ground-state N_2O is $1\sigma^2 2\sigma^2 3\sigma^2 4\sigma^2 5\sigma^2 6\sigma^2 1\pi^4 7\sigma^2 2\pi^4$, $X^1\Sigma^+$. The SCF wavefunctions are derived from a standard [9s5p/5s3p] basis set (Dunning 1971) augmented by 2s ($\alpha = 0.0653$ and $\alpha = 0.0213$), 2p ($\alpha = 0.0449$ and $\alpha = 0.0123$), and 1d ($\alpha = 0.373$) uncontracted functions on the nitrogen centres and 2s ($\alpha = 0.083$ and 0.0237), 2p ($\alpha = 0.0537$ and 0.0133), and 1d ($\alpha = 0.471$) uncontracted functions on the oxygen centre. With this basis set, the calculated SCF energy and the dipole moment, at the experimental equilibrium geometry of the ground state of N_2O ($R_{N-N} = 2.1273$ au and $R_{N-O} = 2.2418$ au) are -183.6964 au and 0.68 Debye, respectively. These results compare well with the corresponding near-Hartree–Fock values of -183.7567 au (McLean and Yoshimine 1967) and 0.64 Debye (Bruns and Person 1970), respectively. The experimental dipole moment is 0.16 Debye (Lovas 1978). The same basis set is also used to calculate the wavefunctions of the $^1\Pi$ and $^3\Pi$ excited states using the improved virtual orbital (IVO, Goddard and Hunt 1974) approximation. These orbitals were obtained by diagonalising the V_{N-1} potential of the frozen-core in the SCF basis. The calculated vertical excitation energies for the transitions to these states at the equilibium geometry of the ground state are 9.294 and 8.921 eV respectively, which can be compared with the values 8.5 and 8.2 eV of Marinković *et al* (1986).

In the SVIM calculations, the continuum wavefuntions are single-centre expanded as

$$\Psi_{\boldsymbol{k}}(\boldsymbol{r}) = (2/\pi)^{1/2}\sum_{lm}\frac{(\mathrm{i})^l}{k}\Psi_{klm}(\boldsymbol{r})Y_{lm}(\hat{k}) \tag{5}$$

where $Y_{lm}(\hat{k})$ are the usual spherical harmonics.

The calculation of $\Psi_{\boldsymbol{k}}(\boldsymbol{r})$ starts with the expansion of the trial functions in a set R_0 of L^2-basis functions $\alpha_i(\boldsymbol{r})$ as follows

$$\tilde{\Psi}_{k,lm}(\boldsymbol{r}) \;=\; \sum_{i=1}^{N} a_{i,lm}(k)\alpha_i(\boldsymbol{r}). \tag{6}$$

Using this basis set, the reactance K-matrix elements can be derived as

$$K^{(R_0)}_{k,ll'm} \;=\; \sum_{i,j=1}^{N}\langle\Phi_{k,l'm} \mid U \mid \alpha_i\rangle[D^{-1}]_{ij}\langle\alpha_j \mid U \mid \Phi_{k,lm}\rangle \tag{7}$$

where $\Phi_{k,lm}$ are the partial-wave free-particle wavefunctions and

$$D_{ij} \;=\; \langle\alpha_i \mid U - UG_0^{(P)}U \mid \alpha_j\rangle. \tag{8}$$

Here, $G_0^{(P)}$ is the principal value of the free-particle Green operator and the zeroth-iteration wavefunction $\Psi_{k,lm}^{R_0}$ is calculated using equation (6) with appropriately calculated coefficients, $a_{i,lm}$. As demonstrated by Lucchese *et al* (1982), the converged scattering solutions can be obtained via an iterative procedure. This procedure consists in augmenting the basis set R_0 by the set

$$S_0 = \{\Psi_{k,l_1m_1}^{(P)^{(R_0)}}(\boldsymbol{r}), \Psi_{k,l_2m_2}^{(P)^{(R_0)}}(\boldsymbol{r}), \ldots \Psi_{k,l_cm_c}^{(P)^{(R_0)}}(\boldsymbol{r})\} \tag{9}$$

where l_c is the maximum value of l for which the expansion of the scattering solution (5) is truncated, and $m_c \leqslant l_c$. A new set of partial wave scattering solutions can now be obtained from

$$\Psi_{k,lm}^{(P)^{(R_1)}}(\boldsymbol{r}) = \Phi_{k,lm}(\boldsymbol{r}) + \sum_{i,j=1}^{M} \langle \boldsymbol{r} \mid G^{(P)}U \mid \eta_i^{(R_1)}\rangle [D^{-1}]_{ij} \langle \eta_j^{(R_1)} \mid U \mid \Phi_{k,lm}\rangle \tag{10}$$

where $\eta_i^{(R_1)}(\boldsymbol{r})$ is any function in the set $R_1 = R_0 \bigcup S_0$ and M is the number of functions in R_1. This iterative procedure continues until a converged $\Psi_{k,lm}^{(P)^{(R_n)}}(\boldsymbol{r})$ is achieved.

We have limited the partial-wave expansions up to $l_c = 17$ and $m_c = 2$. In addition, all matrix elements appearing in the equations (7) and (8) were computed by a single-centre expansion technique with radial integral evaluated using a Simpson quadrature. No additional approximations were used in the calculation of the exchange part of matrix elements. The partial-wave expansions of the direct and exchange parts of potential operator were truncated at $l_d = 29$ and $l_e = 17$, respectively. All the SVIM calculations converged within four iteractions.

For elastic scattering and the transition leading to the $^1\Pi$ state, the partial-wave expansion of the transition T-matrices was also truncated at $l_c = 17$ and $m_c = 2$. Contributions from the higher partial waves were accounted for via the Born-closure procedure. In this procedure, the $B_{m_tm_t'}^{j_t}$ is given by

$$B_{m_tm_t'}^{j_t}(\hat{k}') = B_{m_tm_t'}^{\mathrm{Born},j_t}(\hat{k}') + \sum_{l'lmm'} (-1)^m (\mathrm{i})^{l-l'} (2l+1)^{-1} (T_{ll'mm'}^{S} - T_{ll'mm'}^{\mathrm{Born}}) \times (l-m, l'm' \mid j_t'm_t')(l0, l'm_t \mid j_tm_t) Y_{l'm_t}(\hat{k}'). \tag{11}$$

In equation (5), $B_{m_tm_t'}^{\mathrm{Born},j_t}(\hat{k}')$ is the j_t-basis representation of the Born scattering amplitude, defined as

$$B_{m_tm_t'}^{\mathrm{Born},j_t}(\hat{k}') = \frac{(2j_t+1)}{8\pi^2} \frac{k}{\mathrm{i}\pi^{1/2}} \int \mathrm{d}\hat{R}' f^{\mathrm{Born}}(\hat{R}'; \hat{k}') D_{m_tm_t'}^{j_t*}(\hat{R}') \tag{12}$$

where $D_{m_tm_t'}^{j_t*}(\hat{R}')$ are the usual rotation matrices (Edmonds 1974). The $T_{ll'mm'}^{\mathrm{Born}}$ is the partial-wave Born T-matrix element given by

$$T_{ll'mm'}^{\mathrm{Born}} = \langle S_{klm} \mid U_{st} \mid S_{kl'm'}\rangle \tag{13}$$

where U_{st} is twice the static potential (in atomic units) and S_{klm} are the partial-wave components of the free-particle wavefunction.

On the other hand, for the transition which leads to the $^3\Pi$ state, a direct summation over (lm) which appears in equation (2) is performed. In this case, the truncation parameters used for the DW T-matrix were $l_c = 17$ and $m_c = 5$ for incident energies up to 50 eV. At higher energies, contributions with $l_c = 17$ and $m_c = 9$ were included. In addition, the partial-wave components of the exchange T-matrix with $m \geqslant 3$ were calculated using the undistorted plane waves.

3. Results and discussion

The calculated DCS for elastic electron–N_2O scattering in the 5–80 eV incident energy range are listed in table 1.

Table 1. DCS and ICS (in 10^{-16} cm^2) for elastic electron scattering on N_2O.

Angle	$E_0(eV)$							
(deg)	5	7.5	10	15	20	30	50	80
10	19.61	11.19	11.30	12.94	12.13	13.35	12.86	12.06
20	3.90	3.94	4.94	8.27	7.76	7.35	6.17	4.64
30	4.17	3.66	3.82	5.20	4.70	3.76	2.69	1.89
40	3.77	3.06	2.90	2.94	2.59	1.94	1.32	0.93
50	3.01	2.34	2.17	1.75	1.49	1.14	0.69	0.43
60	2.22	1.70	1.61	1.25	1.00	0.69	0.33	0.25
70	1.52	1.19	1.17	0.97	0.73	0.41	0.19	0.21
80	1.03	0.89	0.90	0.75	0.53	0.35	0.19	0.18
90	0.72	0.74	0.75	0.60	0.44	0.44	0.23	0.17
100	0.59	0.71	0.75	0.58	0.49	0.54	0.26	0.19
110	0.56	0.72	0.78	0.68	0.63	0.59	0.32	0.23
120	0.59	0.73	0.82	0.85	0.79	0.60	0.41	0.29
130	0.65	0.75	0.86	1.04	0.93	0.65	0.54	0.34
140	0.71	0.78	0.96	1.29	1.06	0.77	0.70	0.37
150	0.76	0.83	1.16	1.60	1.20	0.97	0.86	0.40
160	0.80	0.91	1.47	1.94	1.34	1.21	1.03	0.43
170	0.83	0.98	1.73	2.20	1.45	1.39	1.15	0.48
180	0.83	1.01	1.87	2.31	1.50	1.45	1.20	0.50
ICS	23.02	19.25	20.30	21.91	18.86	16.09	12.11	9.06

These results are also shown in figures 1(*a*)–(*d*) and 2(*a*)–(*d*) along with the experimental data when available (Kubo *et al* 1981, Marinković *et al* 1986, Johnstone *et al* 1993). In general, there is a qualitative agreement between our calculated DCS and these measured data. Quantitatively, however, at some incident energies the agreement is good whereas at some other energies, serious discrepancies between the calculated and measured results are seen. For example, at lower incident energies (figure 1(*a*) and (*b*)), the calculated DCS are strongly forward peaked. Although this behaviour is expected for low-energy electron scattering by polar molecules, the comparison with the available experimental data shows that our method strongly overestimates the DCS in this angular region. This discrepancy can be mainly attributed to the neglect of the polarization effects in the calculation, although it can also be partly attributed to the effect of the weak dipole moment of the target. It is well known that the low-energy electron scattering is strongly influenced by such long-range potentials (Machado *et al* 1995a, b).

At higher energies, the agreement between the calculated and measured DCS is considerably better, both qualitatively and quantitatively. The best agreement occurs in the 15–30 eV range, although discrepancies at some intermediate scattering angles are still seen. This disagreement in the middle angular region increases with increasing scattering energy. Since the same behaviour has also been observed in our previous applications of BCSVM to the the study of elastic electron–molecule collisions in the low- and intermediate-energy ranges, it can be shown from the Hartree–Fock description of the target and also the static-exchange approximation used to calculate the electron continuum where the electronic

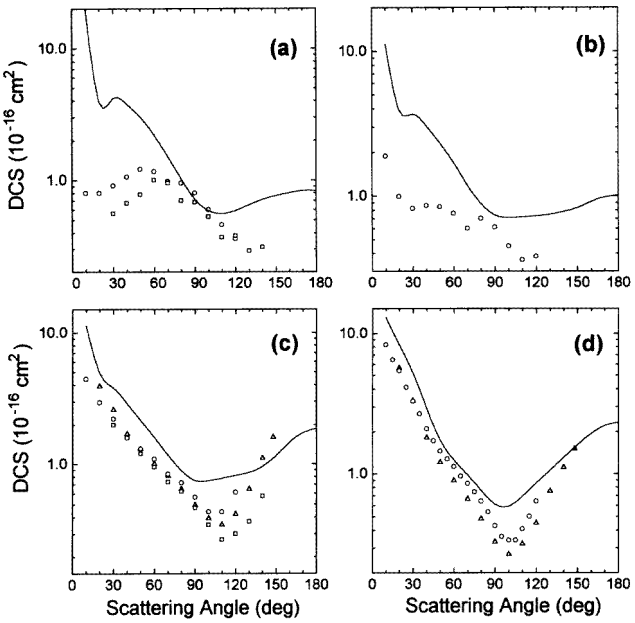

Figure 1. Elastic differential cross sections for e^-–N_2O scattering at (*a*) 5 eV, (*b*) 7.5 eV, (*c*) 10 eV and (*d*) 15 eV. Full curve, present BCSVM results; □, experimental data of Kubo *et al* (1981); △, experimental data of Marinković *et al* (1986); ○ , experimental data of Johnstone *et al* (1993).

correlation effects of the target and between the target and the scattering electron are both neglected.

Figure 3 shows the calculated elastic integral cross sections (ICS) as a function of the incident energy, along with the experimental data of Marinković *et al* (1986) and Johnstone *et al* (1993). Our calculated elastic ICS show a maximum at around 13 eV in agreement with the experimental data of Johnstone *et al* (1993) and of Marinković *et al* (1986). This enhancement of ICS at around 13 eV has been identified, via an eigenphase-sum analysis, as a p-wave ($l = 1$) shape resonance in the $k\sigma$ channel (see the inset of figure 3). Our calculated ICS also show a minimum at around 7 eV. Although there is a strong disagreement between the calculated DCS and experimental data for energies below 10 eV, the existence of a minimum in the experimental ICS of Johnstone *et al* (1993), makes us believe that the minimum in the calculated ICS is physical. The possibility of this minimum being a Ramsauer minimum was discarded. Similar features have also been verified in the elastic electron scattering by H_2S. The possible physical nature of these minima has been discussed previously by Gulley *et al* (1993). At lower energies, our ICS are larger than the experimental data by a factor of 2. Nevertheless, the agreement is considerably better with increasing of incident energy, particularly with the measured data of Marinković *et al* (1986).

In figure 4 we compare the calculated DCS for the transition $X\,^1\Sigma \rightarrow {}^1\Pi$ in N_2O by electron impact at 80 eV with the absolute experimental data of Marinković *et al* (1986). In general, the DW method is able to describe the shape of the experimental DCS, although the positions of the maximum and minimum are shifted relative to the experiment. Quantitatively, the agreement is quite good for scattering angles up to 40^o and larger than

Table 2. DCS and ICS (in $10^{-19}\,cm^2$) for the $X\,^1\Sigma^+ \rightarrow {}^1\Pi(2\pi \rightarrow 8\sigma)$ excitation in N_2O.

Angle	$E_0(eV)$						
(deg)	10	12.5	15	20	30	50	80
10	24.74	68.67	83.38	102.68	121.72	108.76	88.84
20	23.68	65.46	69.88	70.46	64.04	35.76	14.25
30	22.03	59.22	53.51	42.10	27.57	7.57	2.17
40	19.93	50.49	38.10	22.71	10.69	2.74	2.37
50	17.56	40.54	25.60	11.73	4.85	2.81	2.19
60	15.08	30.73	16.44	6.62	3.38	2.76	1.65
70	12.66	22.13	10.28	4.86	3.14	2.28	1.16
80	10.39	15.42	6.49	4.56	3.04	1.72	0.77
90	8.39	10.89	4.46	4.55	2.86	1.31	0.50
100	6.69	8.47	3.65	4.46	2.67	1.07	0.35
110	5.33	7.77	3.63	4.52	2.50	0.92	0.31
120	4.27	8.15	4.05	4.96	2.31	0.82	0.32
130	3.48	8.95	4.69	5.68	2.08	0.76	0.35
140	2.92	9.62	5.41	6.39	1.90	0.74	0.40
150	2.54	9.91	6.10	6.98	1.85	0.73	0.46
160	2.29	9.84	6.70	7.47	1.94	0.71	0.49
170	2.15	9.65	7.12	7.87	2.10	0.67	0.51
180	2.11	9.55	7.27	8.03	2.17	0.66	0.51
ICS	127.1	271.8	186.0	150.0	102.8	59.18	37.24

Table 3. DCS and ICS (in $10^{-19}\,cm^2$) for the $X\,^1\Sigma^+ \rightarrow {}^3\Pi(2\pi \rightarrow 8\sigma)$ excitation in N_2O.

Angle	$E_0(eV)$						
(deg)	10	12.5	15	20	30	50	100
10	3.07	43.88	11.24	18.85	11.77	1.09	1.21
20	3.50	48.66	14.82	23.45	11.88	3.83	2.90
30	4.08	54.44	18.18	26.12	13.46	6.13	1.72
40	4.65	59.08	19.67	24.70	13.81	5.08	1.08
50	5.07	61.16	19.28	20.94	11.96	2.95	1.52
60	5.26	60.48	18.08	18.23	9.57	1.71	1.62
70	5.22	58.05	17.10	18.14	8.10	1.23	1.04
80	5.03	55.77	16.76	18.42	7.57	1.01	0.66
90	4.81	55.46	17.11	19.97	7.46	0.98	0.75
100	4.62	57.95	18.03	19.14	7.58	1.10	0.88
110	4.49	62.41	19.32	18.22	7.96	1.22	0.79
120	4.34	66.65	20.57	18.75	8.33	1.26	0.59
130	4.10	68.29	21.47	20.96	8.29	1.23	0.46
140	3.70	66.05	21.98	23.67	7.98	1.15	0.45
150	3.18	60.42	22.38	25.49	8.23	1.02	0.47
160	2.63	53.48	22.88	25.99	9.58	0.90	0.49
170	2.22	47.86	23.40	25.72	11.36	0.84	0.53
180	2.06	45.72	23.62	25.51	12.19	0.83	0.55
ICS	55.77	745.6	237.7	261.4	115.2	22.70	11.90

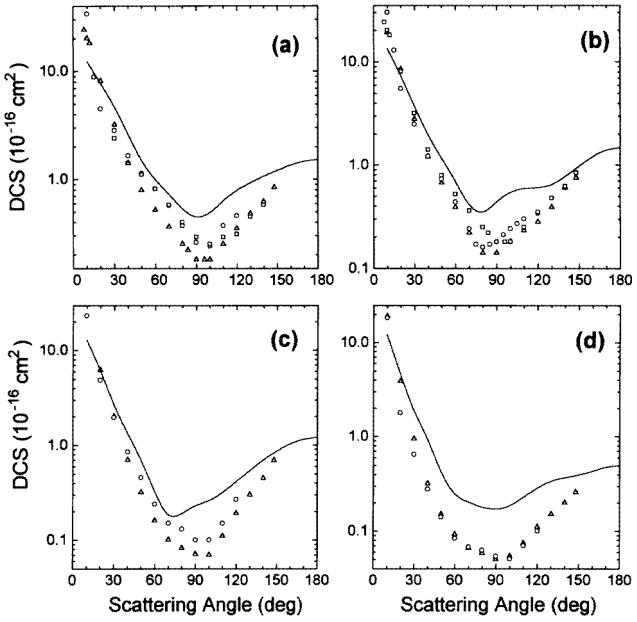

Figure 2. Same as figure 1 at (*a*) 20 eV, (*b*) 30 eV, (*c*) 50 eV and (*d*) 80 eV.

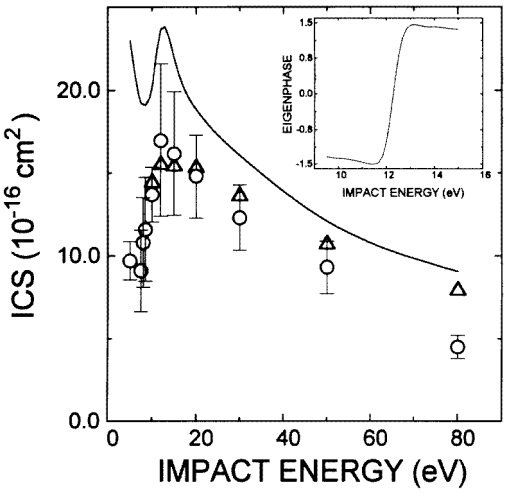

Figure 3. Integral cross sections for elastic electron scattering by N_2O. Full curve, present BCSVM results; △, experimental data of Marinković *et al* (1986); ○ , experimental results of Johnstone *et al* (1993). Inset: the p-wave eigenphases in the $k\sigma$ channel as a function of incident energy.

110°. However, as in elastic scattering, our theory overestimates the DCS at intermediate scattering angles. In figures 5(*a*)–(*c*) we show the calculated DCS for the same transition at the incident energies of 20, 30 and 50 eV, respectively. The relative measurements of Marinković *et al* (1986) normalized to our data at 120° are also shown. At 20 eV, our DW

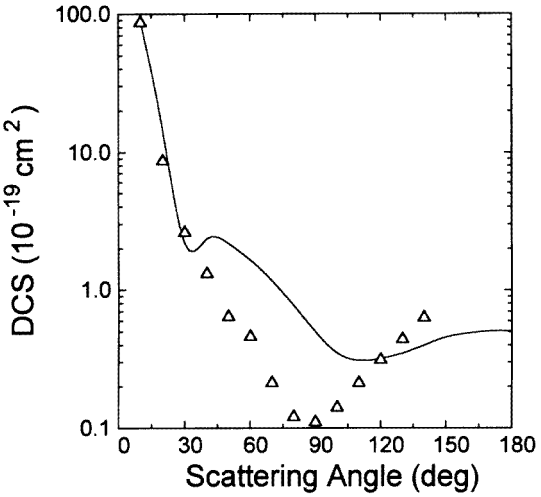

Figure 4. Differential cross sections for the excitation $X^1\Sigma^+ \rightarrow {}^1\Pi(2\pi \rightarrow 8\sigma)$ in N_2O by electron impact at 80 eV. Full curve, present DWA results; △, experimental data of Marinković *et al* (1986).

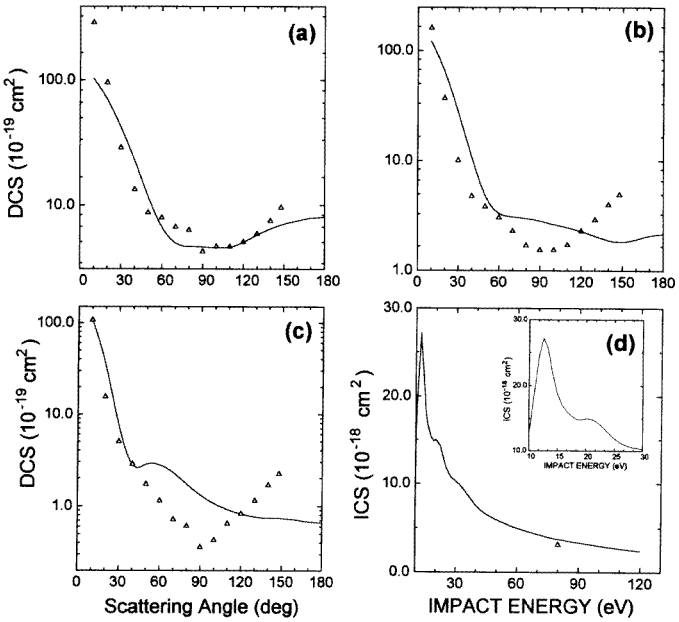

Figure 5. Same as figure 4 at (*a*) 20 eV, (*b*) 30 eV and (*c*) 50 eV. Experimental data are normalized to our calculated results at 120°. (*d*) Integral cross sections for the same transition. Inset: details of ICS in the 10–30 eV range.

results reproduce quite well the shape of the DCS. Again, the agreement between theory and experiment for scattering angles larger than 40° becomes worse with increasing incident energy.

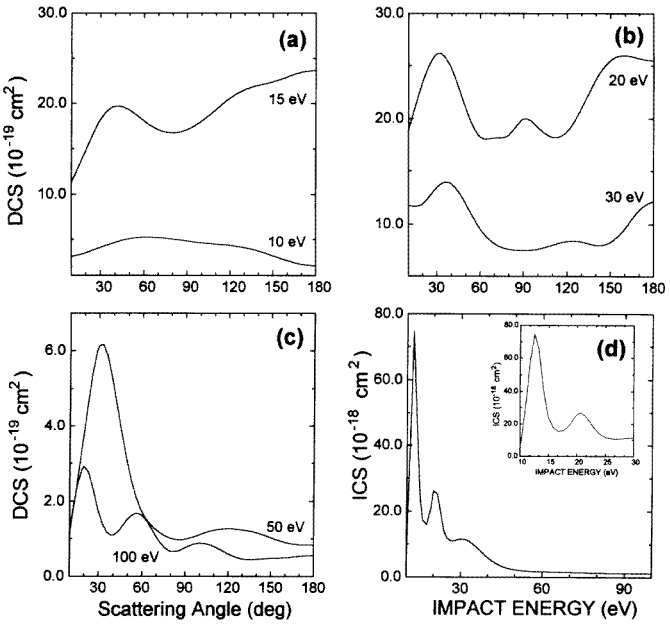

Figure 6. Differential cross sections for the excitation $X^1\Sigma^+ \rightarrow {}^3\Pi(2\pi \rightarrow 8\sigma)$ in N_2O at (*a*) 10 and 15 eV, (*b*) 20 and 30 eV, (*c*) 50 and 100 eV. (*d*) Integral cross sections for the same transition. Inset: details of ICS in the 10–30 eV range.

Figure 5(*d*) shows the calculated ICS for this transition as a function of incident energy. Two resonance features located at around 13 and 21 eV are seen. These maxima in ICS reflect the effect of the same $k\sigma$ p wave shape resonance occurring in the incident and scattered (whose kinetic energy is also around 13 eV) distorted waves, respectively, as discussed for the elastic case. In figure 5(*d*), we also show the only experimental ICS (Marinković *et al* 1986) at 80 eV. The agreement with our calculated result at this energy lies within 20%.

In figures 6(*a*)–(*c*) the DW electron impact excitation DCS for the transition $X^1\Sigma^+ \rightarrow {}^3\Pi$ in N_2O in the incident energy range from 10 to 100 eV are shown. The calculated ICS are shown in figure 6(*d*). For this transition, there are no experimental and theoretical results reported in the literature. Therefore, our results serve as bases of comparison for future investigations. Although the lack of other results seriously limits the discussion, a few comments can still be made. Firstly, two resonance features located at around 13 and 22 eV are also seen. The physical reason for these features is the same as for the transition to the ${}^1\Pi$ state and already discussed above. In addition, one can notice that the oscillations in DCS increase with increasing incident energy. For instance, the maximum of DCS also shifts toward smaller scattering angles. This behaviour was also seen for singlet–triplet types of transitions in other molecules. Also the ICS decrease very rapidly with increasing incident energy, in accordance with such types of transitions.

At some selected energies, the DCS and ICS for the transitions leading to ${}^1\Pi$ and ${}^3\Pi$ states are also listed in tables 2 and 3 respectively. In summary, we present a first theoretical study on the elastic and inelastic electron scattering by N_2O molecules in the low and intermediate energy range. The comparison between the calculated elastic and excitation cross sections and the available experimental data is encouraging. In general, our

theory can reproduce roughly the shape of the DCS although it systematically overestimates the cross sections. The discrepancies are attributed to the Hartree–Fock description of the target and also the neglect of the electron correlation between target and electron continuum.

Acknowledgement

This work is partially supported by Brazilian agencies FINEP-PADCT, CNPq and FAPESP.

References

Andrić L and Hall R 1984 *J. Phys. B: At. Mol. Phys.* **17** 2713
Azria R, Wong S F and Schulz G J 1975 *Phys. Rev.* A **11** 1309
Barnett S M, Mason N J and Newell W R 1991 *Chem. Phys.* **153** 283
Bruns, R E and Person, W B 1970 *J. Chem. Phys.* **53** 1413
Csanak G, Taylor H S and Yaris R, 1971 *Phys. Rev.* A **3** 1322
Dubé L and Herzenberg A 1975 *Phys. Rev.A* **11** 1314
Dunning, T H 1971 *J. Chem. Phys.* **55** 716
Edmonds A R 1974 *Angular Momentum in Quantum Mechanics* (Princeton, NJ: Princeton University) 3rd edn
Fano U and Dill D 1972 *Phys. Rev.* A **6** 185
Fliflet A W and McKoy V 1980 *Phys. Rev.A* **21** 1863
Fox K E and Reid J 1985 *J. Opt. Soc. Am.* B **2** 807
Goddard W A III and Hunt W J 1974 *Chem. Phys. Lett.* **24** 464
Gulley R J, Brunger M J and Buckman S J 1993 *J. Phys. B: At. Mol. Opt. Phys.* **26** 2913
Hahn J and Junge C 1977 *Z. Naturf.* **32a** 190
Johnstone W M and Newell W R 1993 *J. Phys. B: At. Mol. Opt. Phys.* **26** 129
Kubo M, Matsunaga D, Koshio K, Suzuki T and Tanaka H 1981 *Atomic Collision Research in Japan* vol 7, ed Y Hatano *et al* (Tokyo: Society for Atomic Collision Research) Progress Report 4
Kwan Ch K, Hsieh Y-F, Kauppila W E, Smith S J, Stein T S, Uddin M N and Dababneh M S 1984 *Phys. Rev. Lett.* **52** 1417
Lee M-T, Brescansin L M and Lima M A P 1990 *J.Phys.B:At.Mol. Opt.Phys.* **23** 3859
Lee M-T and McKoy V 1983 *Phys. Rev.A* **28** 697
Lee M-T, Brescansin L M, Lima M A P, Machado L E and Leal E P 1990 *J.Phys.B: At.Mol.Opt.Phys.* **23** 4331
Lee M-T, Fujimoto M M, Michelin S E, Machado L E and Brescansin L M 1992 *J. Phys. B: At. Mol. Opt. Phys.* **25** L505
Lee M-T, Michelin S, Kroin T, Machado L E and Brescansin L M 1995 *J.Phys.B: At.Mol.Opt.Phys.* **28** 1859
Lovas, F J 1978 *J. Phys. Chem. Ref. Data* **7** 1628
Lucchese R R, Raseev G and McKoy V 1982 *Phys. Rev.* A **25** 2572
Machado L E, Leal E P, Lee M-T and Brescansin L M 1995a *J. Mol. Structure* (Theochem) **335** 37
Machado L E, Lee M-T, Brescansin L M, Lima M A P and McKoy V 1995b *J.Phys.B: At.Mol.Opt.Phys.* **28** 467
Marinković B, Szmytkowski Cz, Pejčev V, Filipović D and Vuškković I 1986 *J. Phys. B: At. Mol. Opt. Phys.* **19** 2365
McLean A D and Yoshimine M 1967 *Tables of Linear Molecule Wave Functions* ed International Business Machines Corporation, p 195
Rescigno T N, McCurdy C W Jr and McKoy V 1974 *J. Phys. B: At. Mol. Phys.* **7** 2396
Szmytkowski Cz, Maciag K and Karwasz G 1984 *Chem. Phys. Lett.* **107** 481
Szmytkowski Cz, Maciag K, Karwasz G and Filipović D 1989 *J.Phys.B: At.Mol.Opt.Phys.* **22** 525
Trajmar S, Register D F and Chutjian A 1983 *Phys. Rep.* **97** 219
Tronc M, Malegat L, Azria R and Le Coat Y 1981 *Proc. 12th Int. Conf. on Physics of Electronic and Atomic Collisions* ed S Datz (Amsterdam: North-Holland) Abstracts p 372
Wang W and Sze N D 1980 *Nature* **286** 589
Wayne R P 1991 *Chemistry of Atmospheres* 2nd edn (Oxford: Oxford Science Publications)